The Journal of Experimental Biology 210, 454-464
Published by The Company of Biologists 2007
doi:10.1242/jeb.02667

Excitable properties of adult skeletal muscle fibres from the honeybee *Apis mellifera*

Claude Collet* and Luc Belzunces

Ecologie des invertébrés, INRA, Institut National de la Recherche Agronomique, UMR406, Domaine St Paul, Site Agroparc, F-84914 Avignon cedex 9, France

*Author for correspondence (e-mail: claude.collet@avignon.inra.fr)

Accepted 23 November 2006

Summary

In the hive, a wide range of honeybees tasks such as cell cleaning, nursing, thermogenesis, flight, foraging and inter-individual communication (waggle dance, antennal contact and trophallaxy) depend on proper muscle activity. However, whereas extensive electrophysiological studies have been undertaken over the past ten years to characterize ionic currents underlying the physiological neuronal activity in honeybee, ionic currents underlying skeletal muscle fibre activity in this insect remain, so far, unexplored. Here, we show that, in contrast to many other insect species, action potentials in muscle fibres isolated from adult honeybee metathoracic tibia, are not graded but actual all-or-none responses. Action potentials are blocked by Cd^{2+} and La^{3+} but not by tetrodotoxin (TTX) in current-clamp mode of the patch-clamp technique, and as assessed under voltage-clamp, both Ca^{2+} and K^{+} currents are involved in shaping action potentials in single muscle fibres. The activation threshold potential for the voltage-dependent Ca^{2+} current is close to –40 mV, its mean maximal amplitude is –8.5±1.9 A/F and the mean apparent reversal potential is near +40 mV. In honeybees, GABA does not activate any ionic membrane currents in muscle fibres from the tibia, but L-glutamate, an excitatory neurotransmitter at the neuromuscular synapse induces fast activation of an inward current when the membrane potential is voltage clamped close to its resting value. Instead of undergoing desensitization as is the case in many other preparations, a component of this glutamate-activated current has a sustained component, the reversal potential of which is close to 0 mV, as demonstrated with voltage ramps. Future investigations will allow extensive pharmacological characterization of membrane ionic currents and excitation–contraction coupling in skeletal muscle from honeybee, a useful insect that became a model to study many physiological phenomena and which plays a major role in plant pollination and in stability of environmental vegetal biodiversity.

Key words: patch–clamp, skeletal muscle fibre, ion current, insect, honeybee, *Apis mellifera*.

Introduction

Important discoveries concerning axonal conduction, synaptic transmission, integrative neurobiology and behaviour have been made using invertebrates. At the muscle level, invertebrates were also extensively used to explore ultrastructure, excitability, excitation–contraction coupling and contraction (Loesser et al., 1992; Palade and Gyorke, 1993; Takekura and Franzini-Armstrong, 2002). Among invertebrates, the domestic honeybee represents one of the most useful models to study electrical phenomena from the molecular level to the insect society level, owing to (i) the relative simplicity of its neural and neuromuscular systems and (ii) the great complexity and the fine tuning of physiological functions, both of which are needed for the social interactions to take place in the hive (locomotion, thermogenesis, vision, olfaction, communication, learning and memory). The honeybee experimental model is so promising that its genome was recently chosen to be sequenced, giving the model a new dimension with a huge amount of, so far, unexplored data made freely available for the scientific community (http://www.hgsc.bcm.tmc.edu/projects/honeybee/). This insect has a major role to play in scientific research (Menzel et al., 2006; Roberts and Elekonich, 2005; Sattelle and Buckingham, 2006; Whitfield et al., 2002). It is also worthy to mention that honeybee's pollination activity so crucially contributes to vegetal biodiversity stability, that new pesticide compounds must be ascertained to be non-toxic on this law-protected useful insect before being authorized. Over the last ten years, honeybee nervous system electrical activity has been studied at the cellular and molecular level with electrophysiological techniques. A number of ionic currents have been characterized, mainly in neurons from two regions of the honeybee brain: mushroom bodies and antennal lobes (Goldberg et al., 1999; Grunewald, 2003; Kloppenburg et al.,

1999; Laurent et al., 2002; Pelz et al., 1999; Schafer et al., 1994; Wustenberg et al., 2004).

To date, the electrical activity and excitation–contraction coupling of honeybee muscle has remained largely unexplored at the cellular and molecular levels, but work has been done on muscle excitability in other insect species (Pichon and Ashcroft, 1985; Singh and Wu, 1999; Wicher et al., 2001). For instance, since the finding that L-glutamate acts as excitatory neurotransmitter at the neurone-muscle synapse (Kerkut et al., 1965; Usherwood and Machili, 1966), several insect preparations have been used to characterize better neuromuscular transmission in general (for a review, see Osborne, 1996). L-Glutamate causes membrane depolarization if applied iontophoretically at the neuromuscular junction of the *Drosophila* larval muscle fibre (Jan and Jan, 1976a) and the reversal potential of this response as well as the neurally evoked excitatory post-synaptic currents (EPSC) obtained in the locust muscle fibre, both reverse around 0 mV (Anwyl, 1977). Suprathreshold nerve stimulation thus induces a membrane depolarization of the insect skeletal muscle fibre membrane, which is sufficient to trigger, in certain insects, an active all-or none voltage response (spike) which overshoots 0 mV, as for instance is shown in the ventral longitudinal muscle of the flour-moth larva (Deitmer and Rathmayer, 1976) or in the adult *Drosophila* dorsal longitudinal flight muscle (Salkoff and Wyman, 1983). However, at other developmental stages and in several different insect species, some authors showed that only graded voltage responses could be obtained, unless potassium channel blockers where used (for a review, see Pichon and Ashcroft, 1985). Whatever the kinetics of the active membrane potential depolarization (graded or all-or-none), a voltage-dependent calcium entry was found to be responsible for this response. This is the case in skeletal muscle fibres from the locust metathoracic leg (Washio, 1972), the fly dorsal longitudinal flight muscle fibres (Salkoff and Wyman, 1983) and the stick insect ventral longitudinal muscle fibres (Ashcroft, 1981). Various voltage-activated ion currents have also been identified in insect muscle. At least five principal voltage-dependent currents have been described using voltage-clamp techniques: a calcium current, three fast and transient potassium currents (an A-type one and two calcium activated ones) and a delayed potassium outward current (Salkoff, 1983a; Salkoff, 1983b; Salkoff, 1985). Excellent reviews on these ion currents exist (Pichon and Ashcroft, 1985; Singh and Wu, 1999).

Despite the number of valuable studies made on insect neuromuscular transmission and action-potential activity, several points remain to be more thoroughly explored. In the present work, we investigated electrical properties of skeletal muscle fibres with the whole-cell configuration of the patch–clamp technique, taking advantage of an original method to obtain intact isolated skeletal muscle fibres from honeybees. We mainly explored neuromuscular transmission, action potential activity and voltage-dependent calcium entry in these muscle fibres. A preliminary report of some of this work has been presented elsewhere in abstract form (Collet, 2006).

Materials and methods

Single muscle fibre isolation

Experiments were carried out on single muscle fibres enzymatically isolated form the metathoracic tibia (i.e. the third pair of legs) of 1–2 day old honeybees (*Apis mellifera* L.). In the hive, a few hours after emergence, bees have already a substantial amount of their muscles functional as evidenced by the various activities they can perform (e.g. cell cleaning). Bees at day 1 and 2 of adult development were used in order to avoid age-related physiological differences. In order to collect bees at day 1 after emergence, small pieces of capped brood with cells containing 7–9 day old pupae (i.e. at day 18–20 of pre-imaginal development, which lasts 20 days in natural conditions) were taken from the hive and stored in a plastic box placed in a high humidity incubator kept at 28°C. Bees were collected daily and the piece of brood was kept no more than 5 days. For each set of experiments, between five and ten bees were cold-anaesthetized at 4°C and decapitated. Metathoracic tibias were cut out from the legs and stored in a calcium-free Tyrode's solution (see Solutions). The tibia cuticle was then opened longitudinally on one side and pinned open on a flat piece of Sylgard by means of fine minuten pins. Pinned tibias were then enzymatically treated at 37°C under mild agitation for 20 min in a calcium-free Tyrode's solution containing collagenase type 1 (0.5 mg ml^{-1}), pronase E (1 mg ml^{-1}), papain (1 mg ml^{-1}) and trypsin XIII (0.5 mg ml^{-1}). This dissociation solution was specifically adapted to insects from methods designed for mammalian muscles (Collet et al., 1999). Tibias were then rinsed in an enzyme-free Tyrode's solution containing 2 mmol l^{-1} calcium for 15 min. Enzyme-treated muscle mass, loosely attached to cuticle, was removed from each tibia with fine forceps and carefully aspirated with a 1 ml pipette before gentle trituration in a plastic Petri dish filled with calcium-containing Tyrode's solution. The muscle mass of 3–5 tibias were used per dish, yielding sufficient single fibres readily attaching to the bottom of the dish.

Imaging and confocal microscopy

Photographs of the fibres used for patch-clamp experiments were systematically taken under transmitted light with phase contrast objectives (×10 and ×40), using a QICAM camera (Roper Industries Inc., Duluth, GA, USA) attached on the lateral port of an inverted microscope (DMIRB, Leica Microsystems, Wetzlar, Germany). These photographs were used to determine cells morphometric parameters (see Results). In another set of experiments, fibre plasma membrane was stained with the lipophilic cationic membrane dye DI-8-ANNEPS (Molecular Probes, Eugene, OR, USA). This procedure allowed for visualization of the T-tubule network. The dye was first made up as a stock solution of 5 mmol l^{-1} in DMSO and then dissolved at 5 μmol l^{-1} in Tyrode's solution. The dye was continuously present in solution during the whole course of cell observation and imaging with a Bio-Rad confocal microscopy system. In another set of experiments, cells were loaded with the calcium dye Fluo-3-AM at 5 μmol l^{-1} for 30 min at room temperature in Tyrode's solution (a Fluo-3 AM

5 mmol l^{-1} stock solution was first made in DMSO and then dissolved in Tyrode's solution). Cells were imaged with the confocal microscope and Z-stack reconstructions were examined in order to check for the thickness of fibres attaching to the bottom of Petri dishes.

Electrophysiology

An RK-400 patch-clamp amplifier (Bio-Logic, Claix, France) was used in the whole-cell configuration to measure membrane potentials and membrane currents. Command voltage, current pulse generation and data acquisition were done using WinWCP free software (John Dempster, Strathclyde University, UK) driving an A/D, D/A converter (PCI-6014 board, National instruments Corp., Austin, TX, USA). Patch-clamp pipettes were pulled from borosilicate glass capillaries on a vertical pipette puller (P30, Sutter Instrument Co, Novato, AS, USA). The resistance of microelectrodes filled with internal solution (see Solutions) ranged between 1 and 3 MΩ in standard extracellular solutions (Tyrode's solution or tetraethylammonium (TEA)-containing solution). Microelectrode offset potential was nulled prior to seal formation and microelectrode capacitance was zeroed with a fast analogue compensation circuit available on the amplifier, after seal formation, before patch rupture. Tight seal resistance ranged between 1 and 5 GΩ. In whole-cell configuration, the resting holding potential was established at –80 mV. Effective series resistances were compensated at approximately 80%. On average after compensation, series resistance was 0.64±0.05 MΩ (N=41). Cell capacitance was determined by integration of a capacitive transient current elicited by a 10 mV depolarizing pulse from the holding potential after series resistance has been maximally compensated. The area beneath the capacitative transient was used to calculate the cell's linear capacitance. Individual cell capacitance value was used to calculate the density of ionic currents, expressed in terms of amperes per farads (A/F). The mean input resistance was calculated from the steady change in membrane current elicited by a 10 mV depolarizing command step of 20 ms in duration. Voltage-dependent currents were recorded in response to test depolarizations of 100 or 200 ms in duration applied with a 10 mV increment from a holding potential of –80 mV. In order to subtract passive leak currents and linear capacitative currents, each and every test depolarization was preceded by a series of three or four control depolarizations of 10 mV amplitude and 100 ms duration. The average membrane current from these control pulses was appropriately scaled and subtracted from the corresponding test membrane current, supposing a linear evolution of the current with depolarization. Voltage-dependent currents were low pass filtered at 1 kHz and sampled at 10 kHz. In the TEA-containing solution, to ensure that calcium current measurements were accurate, we only used cells in which the voltage drop across the series resistance did not exceed 5 mV. Individual curves of the voltage dependence of the Ca^{2+} current density obtained in the TEA-containing solution, were fitted with Eqn 1:

$$I(V) = G_{max}(V-V_{rev}) / \{1+\exp[(V_{0.5}-V)/k]\} , \quad (1)$$

where $I(V)$ is the peak density of the current for a depolarization to a membrane potential V, G_{max} is the maximum conductance, V_{rev} is the apparent reversal potential, $V_{0.5}$ is the half-activation voltage and k is a steepness factor.

Pressure application of L-glutamate and GABA

Cells were exposed to L-glutamate or GABA by means of a polyethylene capillary perfusion system. Five capillaries were gathered in a common tube, the mouth of which allowed for fast perfusion of the entire cell. The system was pressure driven (0.14×10^5 Pa) and pinch valves were computer-operated (Valvelink 8, Automate Scientific Inc., San Francisco, CA, USA). The maximal amplitude of the glutamate-induced current was measured both at the peak of the current and at the end of the pressure application (t=3 s) at a holding potential of –80 mV. Voltage ramps bringing the membrane potential from –130 mV to +30 mV in 1 s allowed for determination of the glutamate-induced current amplitude over a broad range of potentials (between the ramps, the membrane potential was otherwise held at –80 mV). Recordings were performed using voltage ramps before, during (two ramps starting 2 and 6 s after the onset of glutamate-induced current, respectively) and after a glutamate (1 mmol l^{-1}) application lasting 8 s. The difference between ramps in the presence and in the absence of glutamate was obtained through a point-by-point subtraction and yielded the current–voltage relationship of the glutamate-induced current for each cell.

Solutions

Extracellular Tyrode's solution contained (in mmol l^{-1}): 140 NaCl, 5 KCl, 2 $MgCl_2$, 0 or 2 $CaCl_2$, 10 Hepes, adjusted to pH 7.2 with NaOH. L-glutamate and GABA were dissolved in Tyrode's solution (2 mmol l^{-1} $CaCl_2$). The extracellular TEA-containing solution consisted of (mmol l^{-1}): 140 TEA-$MeSO_3$ (tetraethylammonium-methanesulphonate), 2 $MgCl_2$, 2 $CaCl_2$, 1 4-AP (4-aminopyridine), 10 Hepes, pH 7.2 (adjusted with TEA-OH). Patch pipettes were filled with an internal solution containing: 140 potassium gluconate, 2 $MgCl_2$, 5 EGTA, 10 Hepes, pH 7.2 (adjusted with KOH). Voltages were not corrected for liquid junction potentials, which were calculated to be lower than 5 mV with the different solution tested. EGTA contained in the pipette solution prevented fibre contraction during the protocols used in the experiments described here.

Statistics

Least-square fits were performed using a Levenberg-Marquardt algorithm routine included in Origin (OriginLab Corp., Northampton, MA, USA). Data values are presented as mean ± s.e.m. Statistical significance was determined using a two-tailed t-test assuming P<0.05 as significant.

Results

Cell morphometric data

Fig. 1A shows two typical muscle fibres after the enzymatic dissociation procedure, taken under phase contrast optics

before being patch-clamped in Tyrode's solution (2 mmol l^{-1} $CaCl_2$). In such a solution, only fibres with intact extracellular membrane do not show contracture since uncontrolled calcium entry through holes present in a damaged membrane induce irreversible shortening of the myofibrils. After mechanical dispersion (see Materials and methods), most of the healthy cells were firmly attached to the bottom of the uncoated plastic Petri dish. Fibres from adult honeybee tibial muscles are long and more or less cylindrical (see also confocal microscopy images; Fig. 1F,G). Basement membrane, collagen matrix and tracheoles that lie next to the surface membrane in situ, were digested and/or detached from the cell by the enzymatic treatment, without apparent damage to the membrane. Most of the fibres observed showed fusiform ends although some had rounded ends. Typical sarcomere pattern of A-I bands could be clearly distinguished at this magnification (Fig. 1A). The mean length and width of the cells used for patch-clamp experiments were: 447±15 μm and 27±1 μm (N=41), respectively. The mean sarcomere length was 4.2±0.1 μm (N= 41) in those cells. Observed at a higher magnification under phase contrast transmitted light (Fig. 1B), cells had an accordion-like folded surface membrane, a feature also reported in other adult insects. The depth of this periodic narrowing was more or less pronounced from cell to cell, and was in register with periodic sarcomeres. General cell morphology suggested that enzymatically isolated fibres were healthy. However, our aim being to characterize electrophysiological activity of those fibres, we were also concerned with the ultrastructural integrity of T-tubular membrane network physiologically penetrating within the fibre volume. This part of the cell membrane is critical in the so called 'excitation–contraction coupling' process that takes place in skeletal and heart muscle since it allows for fast and uniform propagation of the electrical signal (i.e. the action potential), leading to calcium entry into the cytoplasm and eventually fibre contraction. After staining of the membrane with DI-8-ANNEPS (see Materials and methods), a nucleus chain interrupting the T-tubule network (double arrow) can be seen in the axial longitudinal confocal section in Fig. 1C, however, a paraxial longitudinal section (Fig. 1D) shows that T-tubules span the entire volume of the fibre, leaving only the central space free of T-tubule membrane. Major sarcolemmal invaginations ('major clefts') typical for arthropod muscle, and well described elsewhere (Huddart and Oates, 1970), can be seen in their transversal section (Fig. 1C, arrow). Those invaginations lead tracheoles through the fibre volume, supplying the cell with air. A double row of T-tubule is seen per sarcomere (well seen in Fig. 1E by comparing the fluorescence profiles taken at ii and iii). A virtual transverse section was reconstructed from a z-stack series of images in one fibre stained with DI-8-ANNEPS (Fig. 1F, Z-stack along the dotted line i shown in Fig. 1D) and another fibre loaded with Fluo3-AM (Fig. 1G). In these two images the more or less cylindrical shape of the cells can be seen. This information was afterwards taken into account in the estimation of the apparent surface of the cell membrane (see below).

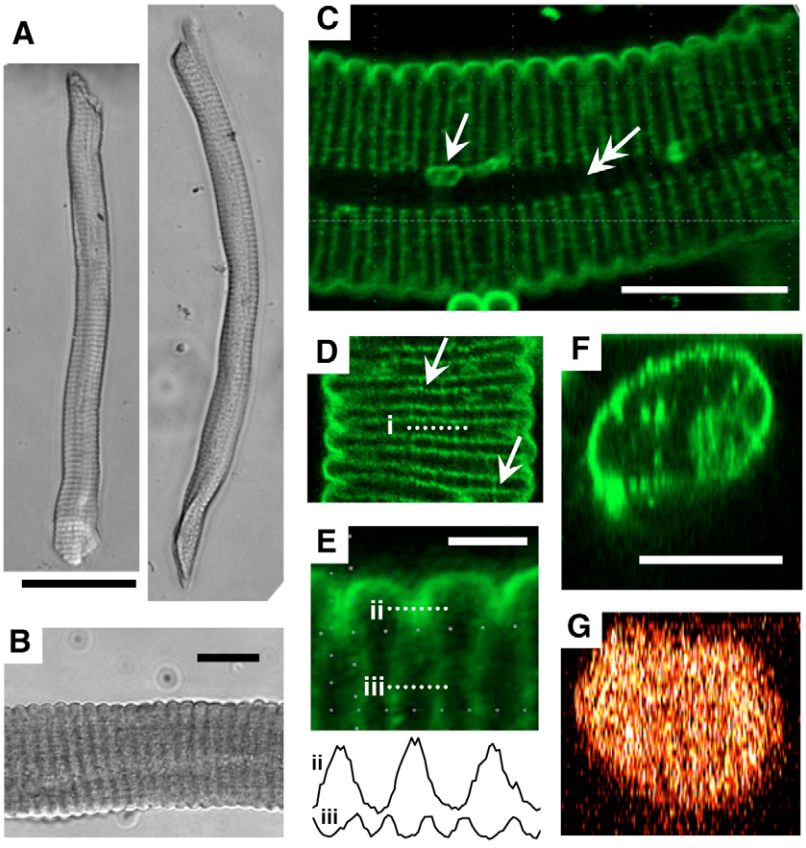

Fig. 1. Single skeletal muscle fibres from adult honeybee leg muscle. (A) Micrographs of two cells bathed in Tyrode's solution taken using phase contrast (transmitted light) microscopy. (B) Part of a cell at a highest magnification, (in horizontal orientation). (C–F) Laser confocal micrographs of T-tubule system in isolated fibres. Single fibres bathed in Tyrode's solution were stained with the lipophilic fluorescent dye di-8 ANEPPS (10 μmol l^{-1}) for 20 min in order to reveal the transverse tubule network. (C) In longitudinal axial section, a central chain of nuclei interrupting T-tubules (double arrow) and tracheoles (arrow) are visible. (D) Longitudinal paraxial section, shows longitudinal connections between T-tubules (arrows) within the same or adjacent sarcomeres. The dotted line (i) shows the position at which the transverse fibre reconstruction shown in F was taken. (E) Continuity of T-tubules with the surface membrane. Two T-tubules per sarcomere penetrate the fibre volume, as emphasized by the profiles of pixel intensity (below) taken at positions ii and iii. (F) Transverse confocal section showing the shape of the fibre. (G) Another cylindrical fibre stained with the calcium fluorophore Fluo-3-AM. Scale bars, 100 μm (A); 20 μm (B); 20 μm (C,D,F,G); 4 μm (E).

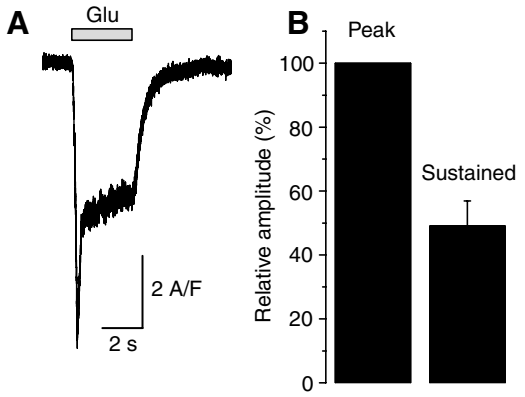

Fig. 2. Glutamate-induced whole-cell currents in voltage-clamped muscle fibres from honeybee. (A) Fast application of L-glutamate (Glu; 1 mmol l^{-1} in Tyrode's solution) through a pressure-driven perfusion system induces a whole-cell inward current consisting of an inactivating initial peak followed by a steady component in one muscle fibre voltage-clamped at –80 mV. The peak and steady component (measured 3 s after the onset of the current) were respectively –7.4 and –3.6 A/F. On average, those values were –7.2±2.0 and –2.2±0.5 A/F (*N*=23 fibres). (B) The mean relative amplitude of the steady component was 49±8% of the initial peak (*N*=23).

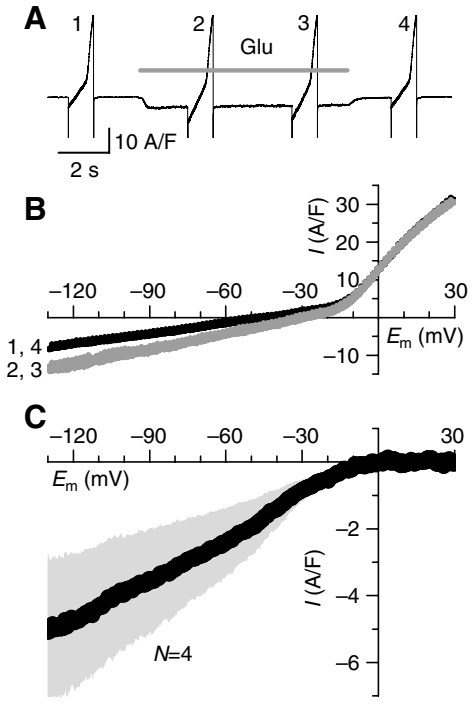

Fig. 3. Current–voltage relationship of the glutamate-induced current in muscle fibres from honeybee. (A) Protocol of voltage ramps running from –130 mV to +30 mV applied before (ramp 1), during (ramps 2 and 3) and after (ramp 4) pressure application of L-glutamate (1 mmol l^{-1} in Tyrode's solution) for 8 s in one muscle fibre otherwise voltage-clamped at –80 mV. Voltage ramps induced activation of voltage-dependent currents and only those with weak voltage-dependent inward calcium current were used for analysis. Application of glutamate induced a current with a sustained inward component (with slow inactivation) at –80 mV. (B) Current–voltage relationships of the whole-cell current obtained in response to the voltage ramps shown in A in the absence (1 and 4, black) or in the presence (2 and 3, grey) of glutamate, show that glutamate elicits an inward component at negative potentials. (C) The mean current–voltage relationship of the glutamate-induced current (*N*=4) appears linear below approx. –20 mV and presents an inward rectification for more positive potential. On the voltage scale considered, the glutamate-induced steady component was null for membrane potentials above approx. 0 mV. The grey shading indicates s.e.m. at each potential explored. E_m, voltage command.

Electrophysiology

Membrane passive properties

The mean capacitance and the mean input resistance of the muscle fibres were 444±29 pF and 31.9±3.2 MΩ, respectively (*N*=41). As shown in the confocal reconstructions of fibre transverse sections (Fig. 1F,G), one can assume a cylindrical geometry of the cells. The apparent fibre surface was then calculated (in cm^2) from individual morphometric fibre measurements and individual values of membrane capacitance (in μF) were used to calculate the individual specific membrane capacitance. On average, the specific membrane capacitance was 1.16±0.06 μF cm^{-2} (*N*=41). This value tends to indicate that the T-tubule membrane system only contributes to a rather small portion of the membrane surface in the fibres studied here. As we will discuss later, this value of specific capacitance could be related to the incomplete maturation of the T-tubule system in developing muscle fibres from newborn bees. Membrane resting potential was measured in nine cells and was –47±5 mV on average in the presence of the calcium-containing Tyrode's solution.

Glutamate-activated currents

In the whole-cell configuration, L-glutamate (1 mmol l^{-1}) applied through a pressure perfusion system induced an inward current at a holding potential of –80 mV (Fig. 2A). A fast activating initial peak inactivating with fast kinetics was observed, followed by a more or less sustained component inactivating slowly. At this glutamate concentration, the initial peak was only clearly seen in half of the cells (11 out of 23 fibres) and its amplitude varied from cell to cell. In the 12 other cells, the fast component was not as obvious, although the initial amplitude of the slowly inactivating response was greater that the late part (3 s after the onset of the response). The peak was measured as the initial amplitude. In the fibre shown in Fig. 2A, the peak and sustained component (measured 3 s after the onset of the current) were –7.4 and –3.6 A/F, respectively. On average, those values were –7.2±2.0 and –2.2±0.5 A/F (*N*=23). The ratio of the sustained amplitude over the peak amplitude was calculated for each fibre. The mean amplitude of the sustained component was 49±8% of the initial peak one (Fig. 2B). In another set of experiments, a voltage-ramp protocol was used in combination with fast

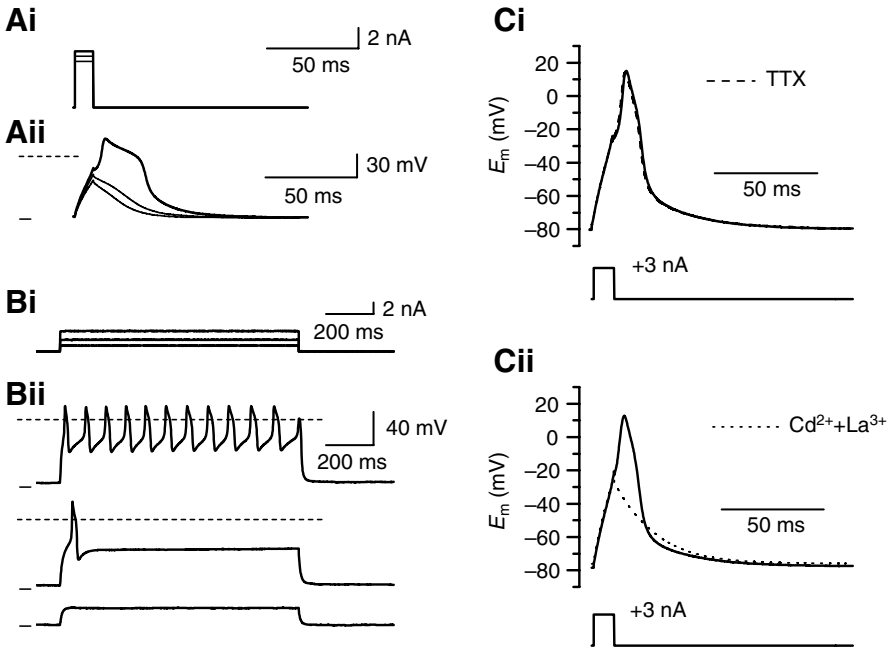

Fig. 4. Action potentials in muscle fibres from honeybee. (A) Three superimposed current steps of 10 ms duration and of increasing amplitude (i) and membrane voltage responses (ii) in a current-clamped muscle fibre bathed in Tyrode's solution (2 mmol l^{-1} $CaCl_2$). The membrane potential was held at –80 mV by passing a constant negative current (minus sign at the beginning of the voltage recordings). Both of the lowest stimulating current steps (a, thin traces) only elicited electrotonic responses. The highest current amplitude (i, thick trace) elicited an action potential overshooting 0 mV (broken line marks the 0 mV level). (B) Three superimposed current steps of 1000 ms duration and of increasing amplitude (i) and the three corresponding membrane voltage responses from bottom to top (ii) in another current-clamped muscle fibre bathed in Tyrode's solution. The membrane potential was held at –80 mV by passing a constant negative current. Whereas the first current step only elicited an electrotonus (ii, bottom trace), the intermediate current step triggered a single action potential (ii, middle trace). The highest current step triggered a train of action potentials (ii, upper trace). (C) In current-clamp, tetrodotoxin (TTX) had no effect on the action potential (upper panel) whereas the calcium channel blockers Cd^{2+} and La^{3+} converted the regenerative action potential response (black line, lower panel) into an electrotonic response (broken line). E_m, voltage command.

perfusion of glutamate to investigate the current–voltage relationship of the sustained component of the glutamate-induced current. Fig. 3A shows the typical protocol used and the membrane current obtained (see Materials and methods) and Fig. 3B shows *I/V* curves in the presence (2 and 3) and in the absence (1 and 4) of glutamate. The mean current-voltage relationship of the glutamate-induced current, obtained from four fibres, is presented in Fig. 3C (s.e.m. is shaded). This relation was approximately linear below –20 mV and started to rectify in the inward direction above this value. Above 0 mV, in the voltage range investigated and for the concentration tested, the sustained component of the glutamate-induced current was null.

Lack of effect of GABA

In our experimental conditions, pressure application of the inhibitory neurotransmitter GABA (γ-amino butyric acid) had no effect at a concentration of 1 mmol l^{-1} on membrane current at a holding potential of –80 mV (*N*=14 fibres, not illustrated). Moreover, voltage ramps indicated that GABA (1 mmol l^{-1}) did not activate any ionic conductance over the voltage range tested (i.e. between –130 and 0 mV, *N*=3 fibres, not shown).

Action potentials

An overshooting spike-like membrane potential response was obtained in response to injection of a positive current under current-clamp in the skeletal muscle fibre from adult honeybee bathed in a solution similar to extracellular fluid (Tyrode's solution 2 mmol l^{-1} $CaCl_2$). Constant current was systematically injected in order to establish a resting membrane potential value around –80 mV. Fig. 4 shows that above a threshold in current step amplitude (Fig. 4Ai; 10 ms in duration, third step), a regenerative voltage response was obtained following a passive electrotonic response and reached values over 0 mV (Fig. 4Aii, broken line) around +20 mV before returning the resting membrane potential (–80 mV, marked by a hyphen). Similar results were obtained in all but one cell (out of seven) tested under these conditions, which responded only with electrotonic responses. Decay phase of the regenerative response followed a complex waveform, including a plateau phase. The plateau phase could be shorter, as shown in Fig. 4C, but no attempt was made to quantify more precisely action potential shape or kinetics characteristics. In the same conditions, but with current steps with a duration increased to 1000 ms, an electrotonic signal was recorded in response to a

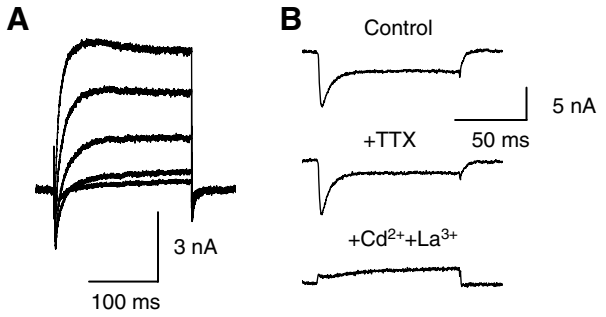

Fig. 5. Whole cell voltage-dependent currents in muscle fibres from honeybee. (A) In voltage-clamp mode, in the presence of Tyrode's solution (2 mmol l^{-1} Ca^{2+}) as the extracellular solution, a series of depolarizations bringing the membrane potential from –80 mV to –30, –10, +10 and +30 mV over a period of 200 ms activated both inward and outward currents. (B) In a fibre depolarized to +10 mV for 100 ms, tetrodotoxin (TTX) had no obvious blocking effect on the inward current (middle trace). However, Cd^{2+} and La^{3+} completely blocked the inward component of the voltage-activated currents (lower trace).

subthreshold current amplitude (Fig. 4Bii, bottom trace). Increasing the current amplitude yielded either a single action potential (Fig. 4Bii, middle trace) or a train of action potentials for the highest stimulation (Fig. 4Bii, upper trace). This feature was recorded in five out of six cells submitted to this stimulation protocol, the remaining one responding with no overshoot but only an electrotonus. Tetrodotoxin (1 μmol l^{-1}) a specific blocker of the voltage-dependent sodium channels was unable to affect action potential (Fig. 4Ci, left panel representative of 3 experiments). However, on the same cell, a single action potential was blocked by Cd^{2+} and La^{3+} applied simultaneously at concentrations of 0.5 and 0.3 mmol l^{-1} respectively (Fig. 4Cii, dashed line, representative of 3 experiments). Similar results were obtained in two other cells.

Voltage-dependent Ca^{2+} and K^+ currents

As expected from current-clamp experiments described above, cells develop inward and outward currents under voltage-clamp conditions. In a representative fibre, from a holding potential of –80 mV, controlled depolarizing pulses of 200 ms in duration and bringing the membrane potential to –20, –10, +10, +20 and +30 mV, induced activation of an inward current followed by an outward current (Fig. 5A). Cd^{2+} and La^{3+} (but not tetrodotoxin; TTX) completely blocked the inward current, as demonstrated in another cell submitted to controlled depolarization to –10 mV (Fig. 5B). This demonstrated unambiguously that in adult honeybee skeletal muscle fibre from tibia, action potential is a phenomenon which depends on activation of voltage-dependent calcium channels but independent of TTX-sensitive voltage-dependent sodium channels. In Tyrode's solution (2 mmol l^{-1} $CaCl_2$), the relative amplitude of voltage-dependant Ca^{2+} and K^+ components varied from fibre to fibre and for instance, while the Ca^{2+} current presented both a peak and maintained net inward component in 11 out of 17 fibres (as seen in Fig. 5B), the remaining fibres only showed a peak but no net maintained component (as seen in Fig. 5A). In order to characterize better the Ca^{2+} inward current, outward potassium currents were blocked by replacing extracellular sodium with TEA and adding the potassium channel blocker 4-AP. Under voltage-clamp conditions, muscle cells were depolarized by steps of 100 ms from a holding potential of –80 mV. Fig. 6A shows that an inward current maintained throughout the depolarizing step developed, and its amplitude increased with depolarization to reach a maximum around 0 mV. The peak and final amplitude of the current (at the end of the depolarizing step) both inversed near +40 mV. Fig. 6B presents the mean current–voltage relationships established for the peak of the current (upper panel, open circles) and the currents at the end of the pulse (lower panel, filled circles). For both peak and end of pulse components, thresholds of activation were around –40 mV and current peaked at 0 mV with mean maximal amplitudes of –8.5±1.9 and –7.0±1.6 A/F, respectively (N=14). For each cell, the current–voltage relationship was fitted using Eqn 1 (see Materials and methods). Mean values for G_{max}, V_{rev}, $V_{0.5}$ and k were 217±36 S/F, +40±4 mV, –13.7±1.8 mV and 5.4±0.5 mV for the peak, and 278±40 S/F, +29±4 mV, –10.5±1.8 mV and 5.7±0.3 mV for the steady state current, respectively.

Discussion

Although a substantial amount of data is currently available on electrical properties of honeybee neurones, this is not the case for skeletal muscle fibres. To our knowledge, our study is the first detailed overview of electrical excitable properties of the honeybee skeletal muscle fibre. Using the whole-cell patch-clamp technique on enzymatically isolated skeletal muscle fibres from honeybee leg, we investigated (i) L-glutamate-induced ionic currents, (ii) action potential activity and (iii) voltage-dependent currents underlying action potential activity. In the past, extracellular recordings have been used as an indicator of honeybee skeletal muscle electrical properties (Bastian and Esch, 1970; Esch and Bastian, 1968; Esch et al., 1975; Kammer and Heinrich, 1972), but we describe here the first characterization of the ionic currents underlying action potential in a skeletal muscle from honeybee under tight control conditions of membrane potential.

In adult skeletal muscle fibres, T-tubules are critical in the propagation of action potential within the volume of the fibre, and staining with a fluorescent lipophilic dye is often a prerequisite in studies dealing with excitability and excitation–contraction coupling in order to reveal this network (Baumann et al., 1990; Kim and Vergara, 1998). Many healthy fibres with an apparently well developed T-tubule network were obtained here. The measured resting potential was in accordance with earlier results obtained in different species (Ashcroft, 1981; Deitmer and Rathmayer, 1976; Washio, 1972). Our results indicate that in skeletal muscle fibres from 1–2-day-old bees, the mean specific membrane capacitance is

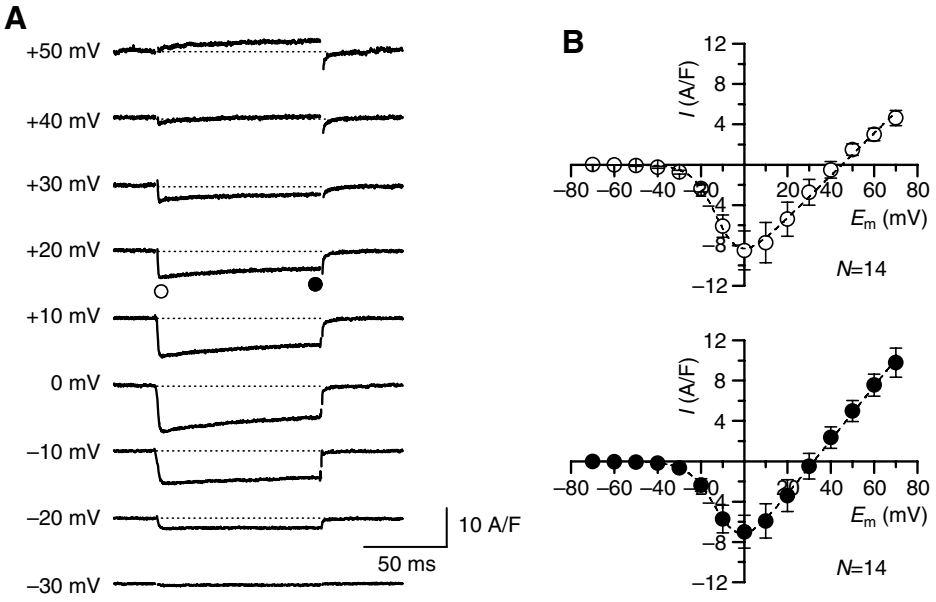

Fig. 6. Calcium currents and corresponding current–voltage relationships in muscle fibres from honeybee. (A) Inward calcium currents were evoked with 100 ms long depolarizing pulses in a voltage-clamped single fibre in the presence of potassium channel blockers, from a holding potential of –80 mV. Open circle, peak of the current; closed circle, end of the depolarization pulse. (B) Mean membrane–current relationship established at the peak of the current (open circles, N=14) and at the end of the depolarization pulses (closed circles). The mean curves were separately fitted using Eqn 1 (see Materials and methods) with values of G_{max}, V_{rev}, $V_{0.5}$ and k of 210 S/F, +45 mV, –10.9 mV and 5.6 mV (upper panel) and 267 S/F, +32 mV, –10 mV and 6 mV (lower panel). E_m, voltage command.

close to 1 μF cm^{-2}, a value reported for membranes lacking an extensive T-tubule network such as neurons (Hodgkin and Huxley, 1952). The highest value that we could obtain was 2.2 μF cm^{-2}. This low value probably does not arise from imperfect space-clamp of the fibre since larval muscle fibres from *Drosophila* (that are very similar to honeybee adult fibres in their dimensions) have been shown to be virtually isopotential (Jan and Jan, 1976b; Wu and Haugland, 1985). In other insect species, the specific membrane capacitance has been calculated with recordings under the two or three microelectrodes voltage-clamp techniques. In adult fibres from locust, stick insect and fly, values ranging from 6.3 to 16.5 μF cm^{-2} have been reported (Kornhuber and Walther, 1987; Pichon and Ashcroft, 1985). However, previous morphometric measurements on mouse skeletal muscle fibres have revealed that the percentage of fibre volume occupied by the T-system increases about fivefold during the first few weeks of postnatal development (Luff and Atwood, 1971). This postnatal increase would explain the low value obtained in muscle from newborn bees. Similarly, the specific membrane capacitance measured with the patch clamp and the two microelectrode voltage-clamp techniques was shown to increase from an average value of 1.5 μF cm^{-2} in fibres from 2-day-old mice to 2.9 μF cm^{-2} in fibres from 44-day-old mice (Beam and Knudson, 1988). The specific capacitance value in fibres from honeybee probably follows the same increase during postnatal development, and one way to determine this would obviously be to assess specific membrane capacitance in muscle fibres from old bees. To date, we were, however, unable to isolate fibres from old bees.

Single fibres from honeybee muscle, plated in a Petri dish, separated from the muscle mass and free from any innervation or trachea represent a valuable preparation to explore the activity of the glutamate receptors involved in insect neuromuscular transmission. We have found that fast application of 1 mmol l^{-1} L-glutamate induced an inward current at the resting membrane potential (–80 mV), lasting for the whole length of perfusion. In approximately half of the fibres, this current was composed of an initial current that peaked and inactivated and of a sustained component. In the remaining fibres, only the sustained component was seen at this glutamate concentration. Voltage ramps tended to indicate that the sustained component was negative below 0 mV and was rectifying inwardly to eventually be null between 0 and +30 mV. In other words, over the voltage range considered, the outward component was seen. Our results are consistent with previous studies performed under voltage-clamp on adult locust muscle fibres showing that (i) the neurally evoked excitatory post-synaptic current (EPSC) and (ii) the current activated by iontophoretic application of L-glutamate at the neuromuscular junction both reverse around 0 mV (Anwyl, 1977). Similar results were obtained under voltage clamp from the *Drosophila* larval (Jan and Jan, 1976a) and adult neuromuscular junctions (Salkoff and Wyman, 1983). Moreover, current–voltage relationships for the responses to nerve stimulation and iontophoretic application of L-glutamate

at the neuromuscular synapse obtained in myotubes from whole *Drosophila* embryo preparations with the patch-clamp technique yielded the same features as those described in our paper. Indeed, the authors showed that the current–voltage relationships for these two kind of responses were both linear below approx. –20 mV, showing inward rectification above this potential, with a current close to 0 pA from approx. –10 to +30 mV [fig. 8A in Broadie and Bate (Broadie and Bate, 1993)]. These authors showed that for potentials more positive than +30 mV, the current becomes outward. As a consequence of this outward rectification, *I*/*V* curves for the two kinds of responses (to nerve stimulation and to iontophoretic application) are N shaped. A closer look at Fig. 6B from (Jan and Jan, 1976a) suggests that this property is also true at the *Drosophila* larva neuromuscular junction. This feature has also been described by others in *Drosophila* larva (N-shaped *I*/*V* curve), although the reversal potential for the synaptic currents was reported higher (above +20 mV), possibly owing to the replacement of potassium with caesium in the patch pipette (Nishikawa and Kidokoro, 1995). Adult insect muscle fibres have both junctional and extrajunctional glutamate receptors (Usherwood and Cull-Candy, 1974). Microelectrode recordings of membrane potential showed that, whereas short iontophoretic application of glutamate at a neuromuscular junction induces a fast transient depolarization of the fibre membrane, such an application at extrajunctional areas induces a biphasic potential response consisting of a fast transient depolarization followed by a slower, prolonged hyperpolarization (Cull-Candy and Usherwood, 1973). The depolarization, so called D-response was reported to result from activation of a cation-selective permeability and is sensitive to the glutamate agonist quisqualic acid. The hyperpolarization, so called H-response was the consequence of a chloride-selective permeability that could be induced by ibotenic acid and was blocked by picrotoxin (for a review, see Osborne, 1996). The physiological significance of the extrajunctional glutamate receptor is unclear but it has been suggested that the circulating concentrations present in hemolymph (extracellular fluid), may act to modulate muscle contractility by reducing the resting input resistance. The two components (initial peak and sustained) obtained here in honeybee fibres could arise from the existence in this preparation of two glutamate receptor subtypes with distinct biophysical properties. Future studies will allow a better characterization of the glutamatergic neuromuscular transmission in honeybee.

GABA failed to induce any ionic current in our voltage-clamp experiments. GABA has been reported to act as inhibitory neurotransmitter at several adult insect neuromuscular synapses. Lack of response in our preparation (muscle fibres from tibia) is, however, not surprising, since it has for example been reported that only less than 20% of the muscle fibres from the locust extensor tibiae (femur muscle) received inhibitory nervous supply (Hoyle, 1978; Usherwood and Grundfest, 1965), even though fibres from specific bundles were also shown to respond to GABA in the absence of inhibitory innervation, thanks to extrajunctional GABA receptors (Cull-Candy, 1986; Cull-Candy and Miledi, 1981). Other insect muscle preparations lacked response to GABA, such as mealworm and fly larva, (Jan and Jan, 1976a; Saito and Kawai, 1985). Similarly, outside-out patches from *Drosophila* larval muscle appeared not to contain GABA-activated channels, even at GABA concentration as high as 10 mmol l^{-1} (Heckmann and Dudel, 1995). Lack of GABA receptors was later confirmed with electrophysiological and immunochemical studies in *Drosophila* larva (Featherstone et al., 2000).

Overshooting action potentials were recorded in honeybee muscle fibres under current clamp. Trains of action potentials were also recorded. Earlier studies showed that similar responses could be recorded in 70% of the fibres in the adult stick insect muscle (Ashcroft, 1981) and 100% of *Drosophila* young adult muscle fibres (Salkoff, 1985). In many other preparations, graded voltage responses were shown to be the physiological responses, and action potentials that were recorded in relatively few fibres could only be seen in the presence of potassium channel blockers (Deitmer, 1977; Washio, 1972). These discrepancies can be explained by species differences, and differential expression of calcium and potassium channels during development (Salkoff, 1985). This has to be related to our voltage-clamp experiments that also showed that relative amplitude of calcium and potassium currents could differ from one fibre to another, although the developmental stages were chosen as homogenously as possible. Experiments showed that in honeybee fibres, the inward current responsible for the rising phase of the action potential is carried by a voltage-dependent calcium channel, since action potentials were blocked by Cd^{2+} and La^{3+} but not by TTX in current-clamp experiments. Similar results were obtained in other preparations (Ashcroft, 1981; Deitmer and Rathmayer, 1976; Rose et al., 2001; Washio, 1972). The Na^{+} channels are absent from our preparation as it is the case in insect muscle fibres in general (Pichon and Ashcroft, 1985). Our study gives a description of the voltage-dependent Ca^{2+} current in tibial muscle from adult honeybee. In the presence of K^{+} channel blockers, membrane depolarizations above –40 mV elicited a Ca^{2+} inward current, which peaked around 0 mV and reversed between +30 and +40 mV. The current activated with fast kinetics, inactivated slowly and was blocked by Cd^{2+} and La^{3+}, but was unaffected by TTX. Similar results have been found in other preparations, such as stick insect muscle and *Drosophila* muscle (Ashcroft and Stanfield, 1982a; Gielow et al., 1995; Salkoff and Wyman, 1983). In the stick insect, a calcium-dependent inactivation of the Ca^{2+} current has been extensively studied (Ashcroft and Stanfield, 1982b), but it was beyond the scope of the present study to investigate in details the biophysical properties of the Ca^{2+} current. However preliminary experiments revealed similar features, and further work will be performed in this area.

In conclusion, the results of the present investigation give insights into the physiology of ionic currents underlying electrical activity in honeybee skeletal muscle fibres. Proper function of muscles and nervous system are necessary in the

hive for any social interactions to take place and perturbation of any of these structures leads to disorganization of the tasks. Future studies will allow further characterization of membrane ionic currents involved in muscle fibre electrical activity and excitation–contraction coupling in this social insect, which plays a major role in plant pollination and in the stability of environmental vegetal biodiversity.

C.C. wishes to thank INRA-SPE scientific department and Région Provence-Alpes-Côte d'Azur for their financial support making it possible to set up a patch-clamp system in Avignon.

References

Anwyl, R. (1977). Permeability of the post-synaptic membrane of an excitatory glutamate synapse to sodium and potassium. *J. Physiol.* **273**, 367-388.

Ashcroft, F. M. (1981). Calcium action potentials in the skeletal muscle fibres of the stick insect *Carausius morosus*. *J. Exp. Biol.* **93**, 257-267.

Ashcroft, F. M. and Stanfield, P. R. (1982a). Calcium and potassium currents in muscle fibres of an insect (*Carausius morosus*). *J. Physiol.* **323**, 93-115.

Ashcroft, F. M. and Stanfield, P. R. (1982b). Calcium inactivation in skeletal muscle fibres of the stick insect, *Carausius morosus*. *J. Physiol.* **330**, 349-372.

Bastian, J. and Esch, H. (1970). The nervous control of the indirect flight muscles of the honey bee. *J. Comp. Physiol. A Neuroethol. Sens. Neural Behav. Physiol.* **67**, 307.

Baumann, O., Kitazawa, T. and Somlyo, A. P. (1990). Laser confocal scanning microscopy of the surface membrane/T-tubular system and the sarcoplasmic reticulum in insect striated muscle stained with DilC18(3). *J. Struct. Biol.* **105**, 154-161.

Beam, K. G. and Knudson, C. M. (1988). Effect of postnatal development on calcium currents and slow charge movement in mammalian skeletal muscle. *J. Gen. Physiol.* **91**, 799-815.

Broadie, K. S. and Bate, M. (1993). Development of the embryonic neuromuscular synapse of *Drosophila melanogaster*. *J. Neurosci.* **13**, 144-166.

Collet, C. (2006). Etude électrophysiologique des courants ioniques macroscopiques de la cellule musculaire squelettique d'abeille adulte par la méthode de patch-clamp. In *Colloque de l'Union Internationale pour l'Etude des Insectes Sociaux (UIEIS), Section Française*. Avignon, France: UIEIS.

Collet, C., Allard, B., Tourneur, Y. and Jacquemond, V. (1999). Intracellular calcium signals measured with indo-1 in isolated skeletal muscle fibres from control and mdx mice. *J. Physiol.* **520**, 417-429.

Cull-Candy, S. G. (1986). Miniature and evoked inhibitory junctional currents and gamma-aminobutyric acid-activated current noise in locust muscle fibres. *J. Physiol.* **374**, 179-200.

Cull-Candy, S. G. and Miledi, R. (1981). Junctional and extrajunctional membrane channels activated by GABA in locust muscle fibres. *Proc. R. Soc. Lond. B Biol. Sci.* **211**, 527-535.

Cull-Candy, S. G. and Usherwood, P. N. (1973). Two populations of L-glutamate receptors on locust muscle fibres. *Nat. New Biol.* **246**, 62-64.

Deitmer, J. W. (1977). Electrical properties of skeletal muscle fibres of the flour moth larva *Ephestia kuehniella*. *J. Insect Physiol.* **23**, 33-38.

Deitmer, J. W. and Rathmayer, W. (1976). Calcium action potentials in larval muscle fibres of the moth *Ephestia kuhniella Z.* (Lepidoptera). *J. Comp. Physiol. A* **112**, 123-132.

Esch, H. and Bastian, J. (1968). Mechanical and electrical activity in the indirect flight muscles of the honey bee. *J. Comp. Physiol. A* **58**, 429-440.

Esch, H., Nachtigall, W. and Kogge, S. N. (1975). Correlations between aerodynamic output, electrical activity in the indirect flight muscles and wing positions of bees flying in a servomechanically controlled wind tunnel. *J. Comp. Physiol. A* **100**, 147-159.

Featherstone, D. E., Rushton, E. M., Hilderbrand-Chae, M., Phillips, A. M., Jackson, F. R. and Broadie, K. (2000). Presynaptic glutamic acid decarboxylase is required for induction of the postsynaptic receptor field at a glutamatergic synapse. *Neuron* **27**, 71-84.

Gielow, M. L., Gu, G. G. and Singh, S. (1995). Resolution and pharmacological analysis of the voltage-dependent calcium channels of *Drosophila* larval muscles. *J. Neurosci.* **15**, 6085-6093.

Goldberg, F., Grunewald, B., Rosenboom, H. and Menzel, R. (1999). Nicotinic acetylcholine currents of cultured Kenyon cells from the mushroom bodies of the honey bee *Apis mellifera*. *J. Physiol.* **514**, 759-768.

Grunewald, B. (2003). Differential expression of voltage-sensitive K^+ and Ca^{2+} currents in neurons of the honeybee olfactory pathway. *J. Exp. Biol.* **206**, 117-129.

Heckmann, M. and Dudel, J. (1995). Recordings of glutamate-gated ion channels in outside-out patches from *Drosophila* larval muscle. *Neurosci. Lett.* **196**, 53-56.

Hodgkin, A. L. and Huxley, A. F. (1952). A quantitative description of membrane current and its application to conduction and excitation in nerve. *J. Physiol.* **117**, 500-544.

Hoyle, G. (1978). Distributions of nerve and muscle fibre types in locust jumping muscle. *J. Exp. Biol.* **73**, 205-233.

Huddart, H. and Oates, K. (1970). Ultrastructure of stick insect and locust skeletal muscle in relation to excitation–contraction coupling. *J. Insect Physiol.* **16**, 1467-1483.

Jan, L. Y. and Jan, Y. N. (1976a). L-glutamate as an excitatory transmitter at the *Drosophila* larval neuromuscular junction. *J. Physiol.* **262**, 215-236.

Jan, L. Y. and Jan, Y. N. (1976b). Properties of the larval neuromuscular junction in *Drosophila melanogaster*. *J. Physiol.* **262**, 189-214.

Kammer, A. E. and Heinrich, B. (1972). Neural control of bumblebee fibrillar muscles during shivering. *J. Comp. Physiol. A* **78**, 337.

Kerkut, G. A., Shapira, A. and Walker, R. J. (1965). The effect of acetylcholine, glutamic acid and GABA on the contractions of the perfused cockroach leg. *Comp. Biochem. Physiol.* **16**, 37-48.

Kim, A. M. and Vergara, J. L. (1998). Supercharging accelerates T-tubule membrane potential changes in voltage clamped frog skeletal muscle fibers. *Biophys. J.* **75**, 2098-2116.

Kloppenburg, P., Kirchhof, B. S. and Mercer, A. R. (1999). Voltage-activated currents from adult honeybee (Apis mellifera) antennal motor neurons recorded in vitro and in situ. *J. Neurophysiol.* **81**, 39-48.

Kornhuber, M. E. and Walther, C. (1987). The electrical constants of the fibres from two leg muscles of the locust *Schistocerca gregaria*. *J. Exp. Biol.* **127**, 173-189.

Laurent, S., Masson, C. and Jakob, I. (2002). Whole-cell recording from honeybee olfactory receptor neurons: ionic currents, membrane excitability and odourant response in developing workerbee and drone. *Eur. J. Neurosci.* **15**, 1139-1152.

Loesser, K. E., Castellani, L. and Franzini-Armstrong, C. (1992). Dispositions of junctional feet in muscles of invertebrates. *J. Muscle Res. Cell Motil.* **13**, 161-173.

Luff, A. R. and Atwood, H. L. (1971). Changes in the sarcoplasmic reticulum and transverse tubular system of fast and slow skeletal muscles of the mouse during postnatal development. *J. Cell Biol.* **51**, 369-383.

Menzel, R., Leboulle, G. and Eisenhardt, D. (2006). Small brains, bright minds. *Cell* **124**, 237-239.

Nishikawa, K. and Kidokoro, Y. (1995). Junctional and extrajunctional glutamate receptor channels in *Drosophila* embryos and larvae. *J. Neurosci.* **15**, 7905-7915.

Osborne, R. H. (1996). Insect neurotransmission: neurotransmitters and their receptors. *Pharmacol. Ther.* **69**, 117-142.

Palade, P. and Gyorke, S. (1993). Excitation-contraction coupling in crustacea: do studies on these primitive creatures offer insights about EC coupling more generally? *J. Muscle Res. Cell Motil.* **14**, 283-287.

Pelz, C., Jander, J., Rosenboom, H., Hammer, M. and Menzel, R. (1999). IA in Kenyon cells of the mushroom body of honeybees resembles shaker currents: kinetics, modulation by K^+, and simulation. *J. Neurophysiol.* **81**, 1749-1759.

Pichon, Y. and Ashcroft, F. M. (1985). Nerve and Muscle: electrical activity. In *Comprehensive Insect Physiology, Biochemistry and Parmacology*. Vol. 5 (ed. G. A. Kerkut and L. Gilbert), pp. 85-113. Oxford: Pergamon Press.

Roberts, S. P. and Elekonich, M. M. (2005). Muscle biochemistry and the ontogeny of flight capacity during behavioral development in the honey bee, *Apis mellifera*. *J. Exp. Biol.* **208**, 4193-4198.

Rose, U., Ferber, M. and Hustert, R. (2001). Maturation of muscle properties and its hormonal control in an adult insect. *J. Exp. Biol.* **204**, 3531-3545.

Saito, M. and Kawai, N. (1985). Developmental changes in the glutamate receptor at the insect neuromuscular synapse. *Brain Res.* **350**, 97-102.

Salkoff, L. (1983a). *Drosophila* mutants reveal two components of fast outward current. *Nature* **302**, 249-251.

Salkoff, L. (1983b). Genetic and voltage-clamp analysis of a *Drosophila* potassium channel. *Cold Spring Harb. Symp. Quant. Biol.* **48**, 221-231.
Salkoff, L. (1985). Development of ion channels in the flight muscles of *Drosophila*. *J. Physiol. Paris* **80**, 275-282.
Salkoff, L. B. and Wyman, R. J. (1983). Ion currents in *Drosophila* flight muscles. *J. Physiol.* **337**, 687-709.
Sattelle, D. B. and Buckingham, S. D. (2006). Invertebrate studies and their ongoing contributions to neuroscience. *Invert. Neurosci.* **6**, 1-3.
Schafer, S., Rosenboom, H. and Menzel, R. (1994). Ionic currents of Kenyon cells from the mushroom body of the honeybee. *J. Neurosci.* **14**, 4600-4612.
Singh, S. and Wu, C. F. (1999). Ionic currents in larval muscles of *Drosophila*. *Int. Rev. Neurobiol.* **43**, 191-220.
Takekura, H. and Franzini-Armstrong, C. (2002). The structure of Ca^{2+} release units in arthropod body muscle indicates an indirect mechanism for excitation-contraction coupling. *Biophys. J.* **83**, 2742-2753.
Usherwood, P. N. and Cull-Candy, S. G. (1974). Distribution of glutamate sensitivity on insect muscle fibres. *Neuropharmacology* **13**, 455-461.
Usherwood, P. N. and Grundfest, H. (1965). Peripheral inhibition in skeletal muscle of insects. *J. Neurophysiol.* **28**, 497-518.
Usherwood, P. N. and Machili, P. (1966). Chemical transmission at the insect excitatory neuromuscular synapse. *Nature* **210**, 634-636.
Washio, H. (1972). The ionic requirements for the initiation of action potentials in insect muscle fibers. *J. Gen. Physiol.* **59**, 121-134.
Whitfield, C. W., Band, M. R., Bonaldo, M. F., Kumar, C. G., Liu, L., Pardinas, J. R., Robertson, H. M., Soares, M. B. and Robinson, G. E. (2002). Annotated expressed sequence tags and cDNA microarrays for studies of brain and behavior in the honey bee. *Genome Res.* **12**, 555-566.
Wicher, D., Walther, C. and Wicher, C. (2001). Non-synaptic ion channels in insects – basic properties of currents and their modulation in neurons and skeletal muscles. *Prog. Neurobiol.* **64**, 431-525.
Wu, C. F. and Haugland, F. N. (1985). Voltage clamp analysis of membrane currents in larval muscle fibers of *Drosophila*: alteration of potassium currents in Shaker mutants. *J. Neurosci.* **5**, 2626-2640.
Wustenberg, D. G., Boytcheva, M., Grunewald, B., Byrne, J. H., Menzel, R. and Baxter, D. A. (2004). Current- and voltage-clamp recordings and computer simulations of Kenyon cells in the honeybee. *J. Neurophysiol.* **92**, 2589-2603.